Gaussian tracking with Kent-distributed direction-of-arrival measurements

Ángel F. García-Fernández, Simon Maskell, Paul Horridge, Jason Ralph

***Abstract*—This paper presents a Gaussian tracking algorithm with direction-of-arrival (DOA) measurements modelled via the Kent distribution. The key aspect of the algorithm is that the Kent distribution directly models the specific characteristics of DOA measurements in the 3-D space, and can account for different uncertainties in azimuth and elevation, which the von Mises-Fisher distribution cannot. At each update step, the algorithm performs iterated statistical linear regressions. We provide two implementations of the algorithms, one based on sigma-points and the other on analytical linearisation. The effectiveness of the approach is evaluated via numerical simulations.**

***Index Terms*—Tracking, direction-of-arrival, Kent-distribution, posterior linearisation.**

I. Introduction

Target tracking and localisation based on noisy direction-of-arrival (DOA) measurements is important in many applications such as advanced vehicular systems, mobile communication systems and sonar [1]–[4]. This problem is usually posed in a Bayesian framework in which the objective is to calculate the posterior density, which refers to the density of the current state given current and past measurements, as it contains all information of interest [5].

In non-linear/non-Gaussian systems, the posterior does not have a closed-form expression and must be approximated. For these systems, it is appealing to develop computationally efficient Gaussian filters, which provide a Gaussian approximation to the posterior with a suitable performance. Examples of these Gaussian filters are the extended Kalman filter (EKF) and sigma-point Kalman filters, e.g. the unscented Kalman filter (UKF) [5], [6].

This paper focuses on the development of Gaussian filters with DOA measurements in a 3-D space. The above-mentioned Gaussian filters can be applied in this scenario by modelling DOA measurements, parameterised by azimuth and elevation angles, as Gaussian densities. However, these methods do not take into account the intrinsic characteristics of angular data [7]. Specifically, the use of standard sums and subtractions, which are required in the update step of the Gaussian filters, can be problematic with angular data [7], [8]. For example, the direct average of the azimuths 170º and -170º is 0º, but it should be 180º [7], and its direct difference is 340º, but it should be 20º. The result is that these Gaussian filters do not work well near azimuth angles close to 180º or DOAs near the poles. A solution to this problem is to perform angular sums and subtractions in sigma-point Kalman filters [9]. Another option to deal with Gaussian DOA measurements is to perform a pseudo-linearisation [10].

While the above methods can work well, their main drawback is to model DOA data with a Gaussian distribution, which is not completely suitable as it is not really a distribution for angular data [7]. A more principled approach is to use a mathematically rigorous probability distribution for directions of arrival, as in the directional statistics discipline [7], and develop Gaussian filters for this type of data. A Gaussian filter with von Mises-Fisher (VMF) distributed measurements was developed in [11]. The VMF distribution properly models DOA measurements but has the disadvantage that the noise in azimuth and elevation must be alike.

In this paper, we address this limitation of the VMF DOA model and propose the modelling of DOA measurements with the Kent distribution [12]–[14]. The Kent distribution is the spherical analogue of the bivariate Gaussian distribution and can model different noise variances in azimuth and elevation. Following [15], we then develop a Gaussian filter based on Kent DOA measurements and statistical linear regression (SLR), for which it is required to use the conditional mean and covariance matrix of the Kent distribution. The use of iterated SLRs in the update generally improves performance of Gaussian filters, especially, for low measurement noise and high nonlinearities [16]. We propose two filter implementations, one based on sigma-points and the other based on first-order Taylor series linearisation.

II. The Kent distribution

Let $S^2 = \left\{z : z^T z = 1, z \in \mathbb{R}^3\right\}$ denote the unit sphere on $\mathbb{R}^3$. The Kent distribution on S^2, also called 5-parameter Fisher-Bingham (FB_5) distribution, has the following parameters: concentration parameter $\kappa \geq 0$, ovalness parameter β, such that $0 \leq \beta < \kappa/2$, and a 3×3 orthonormal matrix $\Gamma = [\gamma_1, \gamma_2, \gamma_3]$ where γ_i is the i-th column vector with $\|\gamma_i\| = 1$. Vector γ_1 represents the mean direction or pole, γ_2 the major axis and γ_3 the minor axis. For $z \in S^2$, the density, w.r.t. the Lebesgue measure in $\mathbb{R}^3$, is [12]

$$\mathcal{K}(z; \kappa, \beta, \Gamma) = \frac{1}{c(\kappa, \beta)} \exp\left(\kappa \gamma_1^T z + \beta\left[\left(\gamma_2^T z\right)^2 - \left(\gamma_3^T z\right)^2\right]\right) \quad (1)$$

The authors are with the Department of Electrical Engineering and Electronics, University of Liverpool, Liverpool L69 3GJ, United Kingdom (emails: {angel.garcia-fernandez, s.maskell, p.horridge, jfralph}@liverpool.ac.uk). A. F. García-Fernández is also with the ARIES Research Centre, Universidad Antonio de Nebrija, Madrid, Spain. The authors would like to thank DSTL Grant no. 1000143726 for financial support.

where the normalising constant is

$$c(\kappa,\beta)=2\pi\sum_{j=0}^{\infty}\frac{\Gamma\left(j+\frac{1}{2}\right)}{\Gamma(j+1)}\beta^{2j}\left(\frac{\kappa}{2}\right)^{-2j-\frac{1}{2}}I_{2j+1/2}(\kappa) \quad (2)$$

where $\mathrm{I}_a(\cdot)$ is the modified Bessel function of the first kind and order a, and $\Gamma(\cdot)$ is the Gamma function. If $\beta=0$, the Kent distribution reduces to the VMF on S^2. A visualisation of (1) for varying κ and β can be found in [13, Fig. 2].

A. Mean and covariance matrix

For notational simplicity, we drop the dependence of $c(\cdot)$ on κ and β, and denote the partial derivatives, evaluated at κ and β, as

$$c_\kappa=\frac{\partial c}{\partial\kappa},\ c_\beta=\frac{\partial c}{\partial\beta},\ c_{\kappa\kappa}=\frac{\partial^2 c}{\partial\kappa^2}. \quad (3)$$

The mean and covariance matrix of the Kent distribution with density (1) are [12], [13]

$$\mathrm{E}[z]=\Gamma\left[\frac{c_\kappa}{c},0,0\right]^T=\frac{c_\kappa}{c}\gamma_1, \quad (4)$$

$$\mathrm{C}[z]=\Gamma\Lambda\Gamma^T, \quad (5)$$

$$\Lambda=\mathrm{diag}\left(\left[\frac{c_{\kappa\kappa}}{c}-\left(\frac{c_\kappa}{c}\right)^2,\frac{c-c_{\kappa\kappa}+c_\beta}{2c},\frac{c-c_{\kappa\kappa}-c_\beta}{2c}\right]\right). \quad (6)$$

To calculate (4) and (5), we first approximate the logarithms of the normalising constant and its derivatives (3) using the methods in [13], [17]. Then, we calculate

$$\frac{c_\kappa}{c}=\exp(\log c_\kappa-\log c),$$
$$\frac{c_{\kappa\kappa}}{c}=\exp(\log c_{\kappa\kappa}-\log c),$$
$$\frac{c_\beta}{c}=\exp(\log c_\beta-\log c),$$

which can be used to obtain (4) and (5). How to improve numerical accuracy for large κ is explained in the Appendix.

III. Gaussian filters with Kent measurements

This section proposes two Gaussian filters with Kent-distributed measurements. The Bayesian update is explained in Section III-A. How to obtain a Gaussian posterior based on linearisation of the measurement is explained in Section III-B. Section III-C explains how to perform SLR for Kent measurements via sigma-points and first order Taylor series. The Gaussian filters resulting from iterated SLRs are explained in Section III-D.

A. Bayesian update

A target state is $x\in\mathbb{R}^{n_x}$ and has a Gaussian prior density

$$p(x)=\mathcal{N}(x;\overline{x},P), \quad (7)$$

where $\mathcal{N}(x;\overline{x},P)$ denotes a Gaussian density with mean $\overline{x}$ and covariance matrix P evaluated at x.

We observe the target with a measurement $z=\left[(z_1)^T,....,(z_m)^T\right]^T$ that consists of m DOA measurements so $z_j\in S^2$ $j=1,2,...,m$. We assume that, given the target state, the measurements are independent so

$$p(z|x)=\prod_{j=1}^{m}p(z_j|x). \quad (8)$$

The DOA measurements follow a Kent distribution

$$p(z_j|x)=\mathcal{K}(z_j;\kappa,\beta,\Gamma_j(x)), \quad (9)$$

$$\Gamma_j(x)=[\gamma_{j,1}(x),\gamma_{j,2}(x),\gamma_{j,3}(x)] \quad (10)$$

where, for simplicity, we have considered that κ and β do not depend on x or j. How to choose $\Gamma_j(x)$ for line-of-sight propagation will be explained in Section IV.

The update step uses Bayes' rule to calculate the posterior

$$p(x|z)\propto p(z|x)\,p(x), \quad (11)$$

where $\propto$ stands for proportionality. There is no closed-form expression for the posterior and it must be approximated.

B. Gaussian filtering

The relation between z_j and x, which is provided by the likelihood (9), can be written as a measurement equation

$$z_j=g_j(x)+\eta_j(x), \quad (12)$$

where $g_j(x)=\mathrm{E}[z_j|x]$, which is a nonlinear transformation of x, and $\eta_j(x)$ is a zero-mean noise with covariance matrix $R_j(x)=\mathrm{C}[z_j|x]$ conditioned on x. Noise $\eta_j(x)$ is uncorrelated with x and $g_j(x)$.

The conditional moments $g_j(x)=\mathrm{E}[z_j|x]$ and $R_j(x)=\mathrm{C}[z_j|x]$ are

$$g_j(x)=\frac{c_\kappa}{c}\gamma_{j,1}(x), \quad (13)$$

$$R_j(x)=\Gamma_j(x)\,\Lambda\Gamma_j^T(x). \quad (14)$$

In order to obtain a Gaussian filter for the Kent-distributed measurements, we perform a linearisation [15], [16]

$$z_j\approx A_jx+b_j+r_j, \quad (15)$$

where $A_j\in\mathbb{R}^{3\times n_x}$, $b_j\in\mathbb{R}^3$ and r_j is a zero-mean noise with covariance matrix $\Omega_j\in\mathbb{R}^{3\times3}$, uncorrelated with x.

Under the assumption that r_j is Gaussian, the posterior becomes Gaussian with mean and covariance matrix

$$\overline{u}=\overline{x}+PA^T\left(APA^T+\Omega\right)^{-1}(z-A\overline{x}-b), \quad (16)$$

$$W=P-PA^T\left(APA^T+\Omega\right)^{-1}AP, \quad (17)$$

where $A=\left[A_1^T,....,A_m^T\right]^T$, $b=\left[b_1^T,....,b_m^T\right]^T$ and $\Omega=\mathrm{diag}(\Omega_1,...,\Omega_m)$. The accuracy of the approximated posterior only depends on how we choose A,b and Ω.

C. Statistical linear regression

SLR is key to making a suitable choice of A,b and Ω. In a general setting, given a prior density $p(\cdot)$ on x with mean $\overline{x}$ and covariance matrix P, SLR finds the best affine

approximation, represented by $\left(A_j^+, b_j^+\right)$, between z_j and x [15]

$$\left(A_j^+, b_j^+\right) = \underset{(A_j, b_j)}{\arg\min} \, \mathrm{E}\left[\left\|g_j(x) + \eta_j(x) - A_j x - b_j\right\|^2\right] \tag{18}$$

$$= \underset{(A_j, b_j)}{\arg\min} \, \mathrm{E}\left[\left\|g_j(x) - A_j x - b_j\right\|^2\right] \tag{19}$$

where the expectation is taken w.r.t. $p(\cdot)$. We have

$$A_j^+ = \mathrm{C}\left[x, g_j(x)\right]^T P^{-1}, \tag{20}$$

$$b_j^+ = \mathrm{E}\left[g_j(x)\right] - A_j^+ \overline{x}. \tag{21}$$

The resulting mean square error matrix is

$$\Omega_j^+ = \mathrm{C}\left[g_j(x)\right] + \mathrm{E}\left[R_j(x)\right] - A_j^+ P \left(A_j^+\right)^T. \tag{22}$$

Therefore, in order to obtain the SLR, we need to calculate the moments $\mathrm{E}\left[g_j(x)\right]$, $\mathrm{E}\left[R_j(x)\right]$, $\mathrm{C}\left[x, g_j(x)\right]$ and $\mathrm{C}\left[g_j(x)\right]$, where $g_j(\cdot)$ and $R_j(\cdot)$ are given by (13) and (14). These moments can be approximated using sigma-points and first-order Taylor series, see Algorithms 1 and 2.

Algorithm 1 SLR using sigma-points

Input: Parameters κ and β, function $\Gamma_j(\cdot)$, and the first two moments $\overline{x}$, P of a density $p(\cdot)$.
Output: SLR parameters $\left(A_j^+, b_j^+, \Omega_j^+\right)$.
- Select m_s sigma-points $\mathcal{X}_1, \ldots, \mathcal{X}_{m_s}$ and weights $\omega_1, \ldots, \omega_{m_s}$ according to $\overline{x}$ and P [5].
- Transform the sigma-points $\mathcal{H}_i = \Gamma_j(\mathcal{X}_i) \quad i = 1, \ldots, m_s$, where $\mathcal{H}_i \in \mathbb{R}^{3\times 3}$ and $\mathcal{H}_i^1$ denotes its first column.
$\mathrm{E}\left[g_j(x)\right] \approx \frac{c_\kappa}{c} \sum_{i=1}^{m_s} \omega_i \mathcal{H}_i^1$.
$\mathrm{E}\left[R_j(x)\right] \approx \sum_{i=1}^{m_s} \omega_i \mathcal{H}_i \Lambda \left(\mathcal{H}_i\right)^T$.
$\mathrm{C}\left[x, g_j(x)\right] \approx \sum_{i=1}^{m_s} \omega_i \left(\mathcal{X}_i - \overline{x}\right)\left(\frac{c_\kappa}{c}\mathcal{H}_i^1 - \mathrm{E}\left[g_j(x)\right]\right)^T$.
$\mathrm{C}\left[g_j(x)\right] \approx \sum_{i=1}^{m_s} \omega_i \left(\frac{c_\kappa}{c}\mathcal{H}_i^1 - \mathrm{E}\left[g_j(x)\right]\right)\left(\frac{c_\kappa}{c}\mathcal{H}_i^1 - \mathrm{E}\left[g_j(x)\right]\right)^T$.
- Calculate A_j^+, b_j^+, Ω_j^+ using (20), (21) and (22).

Algorithm 2 SLR using first-order Taylor series

Input: Function $\Gamma_j(\cdot)$, Jacobian $\nabla\gamma_{j,1}(\cdot)$ (see (10)), parameters κ and β, and the first two moments $\overline{x}$, P of a density $p(\cdot)$.
Output: SLR parameters $\left(A_j^+, b_j^+, \Omega_j^+\right)$.
$\mathrm{E}\left[g_j(x)\right] \approx \frac{c_\kappa}{c}\gamma_{j,1}(\overline{x})$, see (10).
$\mathrm{E}\left[R_j(x)\right] \approx \Gamma_j(\overline{x}) \Lambda \Gamma_j^T(\overline{x})$.
$\mathrm{C}\left[x, g_j(x)\right] \approx \frac{c_\kappa}{c} P \left(\nabla\gamma_{j,1}(\overline{x})\right)^T$.
$\mathrm{C}\left[g_j(x)\right] \approx \left(\frac{c_\kappa}{c}\right)^2 \nabla\gamma_{j,1}(\overline{x}) P \left(\nabla\gamma_{j,1}(\overline{x})\right)^T$.
- Calculate A_j^+, b_j^+, Ω_j^+ using (20), (21) and (22).

D. Gaussian update via iterated SLRs

This section explains how to approximate the posterior moments (16) and (17) using iterated SLRs with respect to the posterior. In Gaussian filtering, a usual way to obtain a Gaussian approximation to the posterior is to calculate A, b and Ω using SLR w.r.t. the prior (as in sigma-point Kalman filters) or using a first-order Taylor series linearisation around $\overline{x}$ (as in the extended Kalman filter). For additive Gaussian measurement noise, the Kullback Leibler divergence shows that this type of approximation is not accurate for sufficiently high nonlinearities in relation to the measurement noise covariance matrix [18].

One can improve performance using an iterative procedure in which we refine the selection of A, b and Ω at each step, by performing SLR w.r.t. the current approximation of the posterior. That is, ideally, we would like to perform the SLR in the area where the posterior has its mass [11], [16]. In practice, we start by calculating A_j^1, b_j^1, Ω_j^1 using SLR w.r.t. $\overline{u}^1 = \overline{x}$, $W^1 = P$ for all measurements. The posterior moments at step 2, $\overline{u}^2$ and W^2, are obtained by substituting A_j^1, b_j^1, Ω_j^1 for $j = 1, ..., m$ into (16) and (17), without changing $\overline{x}$ and P. Now, we perform SLR w.r.t. $\overline{u}^2$ and W^2 to obtain A_j^2, b_j^2, Ω_j^2. The iterations stop after a fixed number or with a convergence criterion [11, Alg. 3]. The steps of the resulting iterated posterior linearisation filter (IPLF) update are indicated in Algorithm 3.

Algorithm 3 IPLF update with DOA Kent measurements

Input: Prior moments $\overline{u}^1 = \overline{x}$, $W^1 = P$, measurements $z_1, \ldots, z_m$, parameters κ and β, function $\Gamma_j(\cdot)$ and number J of iterations.
Output: Posterior moments $\overline{u}^{J+1}$, W^{J+1}.
for $i = 1$ to J **do**
  for $j = 1$ to m **do**
    - Obtain A_j^i, b_j^i, Ω_j^i via SLR w.r.t. $\overline{u}^i$, W^i:
      - For sigma-point implementation, run Algorithm 1.
      - For Taylor series implementation, run Algorithm 2.
  end for
  - Compute $\overline{u}^{i+1}$, W^{i+1} using (16) and (17) with
    - $A = \left[\left(A_1^i\right)^T, ..., \left(A_m^i\right)^T\right]^T$, $b = \left[\left(b_1^i\right)^T, ..., \left(b_m^i\right)^T\right]^T$,
    - $\Omega = \mathrm{diag}\left(\Omega_1^i, ..., \Omega_m^i\right)$.
end for

IV. Direction-of-arrival measurement modelling

This section explains how to model Kent-distributed DOA measurements based on line-of-sight propagation to be able to apply the algorithms developed in Section III to tracking with DOA measurements. This requires the specification of the parameters of the Kent distribution: $\Gamma_j(\cdot)$, κ and β.

In Section IV-A we explain how to choose $\Gamma_j(\cdot)$. In Section IV-B, we explain the relation between the Kent distribution and the Gaussian distribution. This enables us to choose κ and β based on the variances in azimuth and elevation of the measurement, which are related to the antenna beam-width.

A. Choice of $\Gamma_j(\cdot)$ for line-of-sight propagation

Given a target state x, we need $\Gamma_j(x)$ to obtain $p(z_j|x)$, see (9). Let us consider a target moving in a 3D space such that $x = [p_x, v_x, p_y, v_y, p_z, v_z]^T$, where $[p_x, p_y, p_z]^T$ is the position vector and $[v_x, v_y, v_z]^T$ is the velocity vector. For a sensor j located at $[s_{x,j}, s_{y,j}, s_{z,j}]^T$ that measures DOA with straight line propagation, the true azimuth and elevation are

$$\varphi_j^x = \mathrm{atan2}\left(p_y - s_{y,j}, p_x - s_{x,j}\right), \tag{23}$$

$$\theta_j^x = \arcsin\left(\frac{p_z - s_{z,j}}{\left\|[p_x - s_{x,j}, p_y - s_{y,j}, p_z - s_{z,j}]\right\|}\right). \tag{24}$$

Then, matrix $\Gamma_j(x)$ in (9) is given by

$$\Gamma_j(x) = R_z\left(\varphi_j^x\right) R_y\left(\theta_j^x\right) \tag{25}$$

where

$$R_z\left(\varphi_j^x\right) = \begin{bmatrix} \cos\varphi_j^x & -\sin\varphi_j^x & 0 \\ \sin\varphi_j^x & \cos\varphi_j^x & 0 \\ 0 & 0 & 1 \end{bmatrix}, \tag{26}$$

$$\cos\varphi_j^x = \frac{p_x - s_{x,j}}{\|[p_x - s_{x,j}, p_y - s_{y,j}]\|}, \tag{27}$$

$$\sin\varphi_j^x = \frac{p_y - s_{y,j}}{\|[p_x - s_{x,j}, p_y - s_{y,j}]\|}, \tag{28}$$

is a rotation of an angle φ_j^x around the z-axis and

$$R_y\left(\theta_j^x\right) = \begin{bmatrix} \cos\theta_j^x & 0 & -\sin\theta_j^x \\ 0 & 1 & 0 \\ \sin\theta_j^x & 0 & \cos\theta_j^x \end{bmatrix}, \tag{29}$$

$$\cos\theta_j^x = \frac{\|[p_x - s_{x,j}, p_y - s_{y,j}]\|}{\|[p_x - s_{x,j}, p_y - s_{y,j}, p_z - s_{z,j}]\|}, \tag{30}$$

$$\sin\theta_j^x = \frac{p_z - s_{z,j}}{\|[p_x - s_{x,j}, p_y - s_{y,j}, p_z - s_{z,j}]\|}, \tag{31}$$

is a rotation of an angle $-\theta_j^x$ around the y-axis.

Plugging (26) and (29) into (25), we obtain

$$\Gamma_j(x) = \begin{bmatrix} \cos\varphi_j^x\cos\theta_j^x & -\sin\varphi_j^x & -\cos\varphi_j^x\sin\theta_j^x \\ \sin\varphi_j^x\cos\theta_j^x & \cos\varphi_j^x & -\sin\varphi_j^x\sin\theta_j^x \\ \sin\theta_j^x & 0 & \cos\theta_j^x \end{bmatrix}. \tag{32}$$

The resulting Kent distribution corresponds to the rotation $\Gamma_j(x)$ of a Kent distribution with $\Gamma = I_3$, which points at $[1,0,0]^T$ and has the major axis parallel to the xy-plane.

B. Relation with the Gaussian distribution

The most commonly used distribution to model DOA measurements is the Gaussian distribution. In this section, we provide the link between the two distributions, and illustrate the advantages of the Kent distribution to model DOA measurements. For $\Gamma = I_3$, the density (1) takes a simplified form

$$\mathcal{K}(z;\kappa,\beta,I_3) = \frac{1}{c(\kappa,\beta)}\exp\left(\kappa z_1 + \beta\left[z_2^2 - z_3^2\right]\right) \tag{33}$$

where $z = [z_1, z_2, z_3]^T$.

Changing variables to spherical coordinates (φ,θ) with $0 \leq \varphi < 2\pi$ and $-\pi/2 \leq \theta \leq \pi/2$, such that

$$z = [\cos\varphi\cos\theta, \sin\varphi\cos\theta, \sin\theta]^T,$$

we have

$$\mathcal{K}(\varphi,\theta;\kappa,\beta,I_3) = \frac{1}{c(\kappa,\beta)}\exp\left(\kappa\cos\varphi\cos\theta + \beta\left[\sin^2\varphi\cos^2\theta - \sin^2\theta\right]\right). \tag{34}$$

We can then use a Laplace approximation to obtain a Gaussian approximation to (34) [19]. The Taylor series up to second order of the logarithm of (34) around the maximum $(\varphi,\theta) = (0,0)$ provides

$$\log\mathcal{K}(\varphi,\theta;\kappa,\beta,I_3) \approx -\log c(\kappa,\beta) + \kappa - \frac{1}{2}(\kappa - 2\beta)\varphi^2 - \frac{1}{2}(\kappa + 2\beta)\theta^2. \tag{35}$$

Therefore, the Gaussian approximation becomes [20]

$$\mathcal{K}(\varphi,\theta;\kappa,\beta,I_3) \approx \mathcal{N}\left(\varphi;0,\frac{1}{\kappa - 2\beta}\right)\mathcal{N}\left(\theta;0,\frac{1}{\kappa + 2\beta}\right). \tag{36}$$

This approximation becomes more accurate for large κ and β with $0 \leq \beta < \kappa/2$. It should also be noted that the elevation variance is smaller or equal than the azimuth variance.

Therefore, for a Gaussian DOA model centered at $(0,0)$ with variances σ_φ^2 and σ_θ^2 in azimuth and elevation ($\sigma_\theta^2 \leq \sigma_\varphi^2$), the corresponding κ and β for (33) are

$$\kappa = \frac{1}{2}\left(\frac{1}{\sigma_\varphi^2} + \frac{1}{\sigma_\theta^2}\right), \quad \beta = \frac{1}{4}\left(\frac{1}{\sigma_\theta^2} - \frac{1}{\sigma_\varphi^2}\right). \tag{37}$$

Equation (37) enables us to select κ and β based on σ_φ^2 and σ_θ^2, which are related to antenna beam-width. If we have a sensor with $\sigma_\theta^2 > \sigma_\varphi^2$, we make a rotation of 90° around the x axis to the Kent distribution (33), such that it becomes Kent-distributed with parameters κ, β and

$$\Gamma = R_x(\pi/2),\ R_x(\alpha) = \begin{bmatrix} 1 & 0 & 0 \\ 0 & \cos\alpha & -\sin\alpha \\ 0 & \sin\alpha & \cos\alpha \end{bmatrix}.$$

By proceeding analogously to the case $\Gamma = I_3$, we can obtain a Gaussian approximation around $(\varphi,\theta) = (0,0)$ to obtain (36), but with azimuth and elevation interchanged.

To sum up, for large κ and β, and the mode located at $[1,0,0]^T$, or more generally, on the xy plane, the Kent and Gaussian distributions behave similarly. However, important differences arise if the mode is at a different elevation, as illustrated in the following example.

Example 1. We consider a Kent distribution with κ and β corresponding to azimuth and elevation variances, $\sigma_\varphi^2 = (5\pi/180)^2$ and $\sigma_\theta^2 = (2\pi/180)^2$, see (37). We obtain 10000 samples from this distribution with mode at 0º/0º (azimuth-elevation), which corresponds to $\Gamma = I_3$, and with mode at 0º/85º, whose Γ is obtained with (25). The samples[1] are shown in Figure 1 (top). Changing the elevation of the mode implies a rotation in the distribution. We show 10000 samples from Gaussian distributions on azimuth/elevation with the same means and variances in Figure 1 (bottom). For 0º elevation, the Kent and Gaussian distributions are quite similar, as shown in this section. For 85º elevation, the Gaussian distribution undergoes a major transformation w.r.t. 0º elevation. The Kent distribution is a more accurate model for directional antennas.

V. Simulations

This section analyses the performance of the proposed algorithms in relation to other relevant filters in the literature. We refer to the proposed filters with J iterations as K-IPLFJ for the sigma-point implementation and K-IPLFJ (T) for the first-order Taylor series implementation[2] [16]. We have also implemented the UKF for DOA measurements in [9], which

[1]We have used the 3D-Directional-SSV package to sample the Kent distribution: https://github.com/TerdikGyorgy/3D-Simulation-Visualization.

[2]Matlab code will be available at https://github.com/Agarciafernandez.

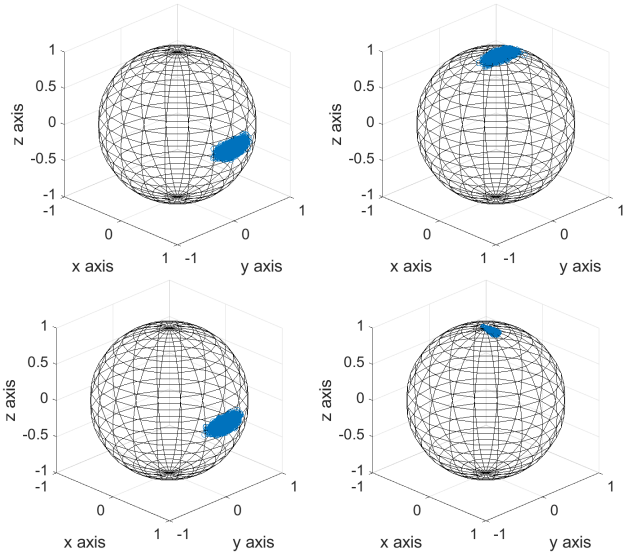

Figure 1: Samples from Kent (top) and Gaussian (bottom) distributions with mode at 0º/0º (azimuth-elevation) (left) and at 0º/85º (right), see Example 1. The Gaussian distribution has azimuth and elevation variances $\sigma_\varphi^2 = (5\pi/180)^2$ and $\sigma_\theta^2 = (2\pi/180)^2$ and the Kent distribution matches these variances for 0º elevation. For 0º elevation, the Kent and the Gaussian distribution are quite similar. For 85º elevation, the Kent distribution is simply a rotation of the Kent distribution at 0º, as would happen for a directional antenna that is now pointing upwards. On the contrary, there is a major change in the shape of the Gaussian distribution.

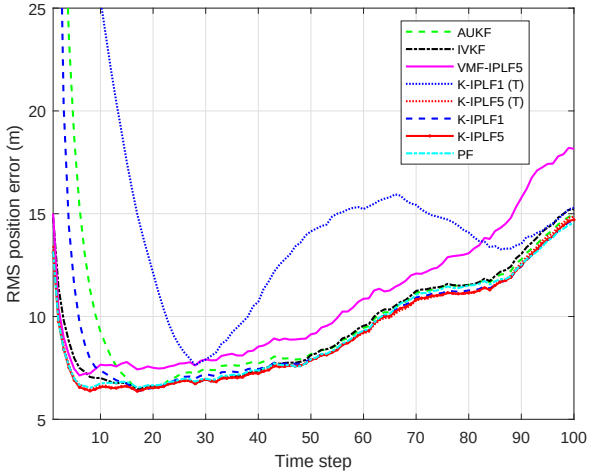

Figure 2: RMS position errors against time. K-IPLF5 and K-IPLF5(T) are the best performing filters. The iterated versions of the algorithms are specially beneficial at the first update due to the large uncertainty in the prior.

is referred to as angular UKF (AUKF). We also consider the IPLF with VMF measurements (VMF-IPLFJ) [11]. These filters use the unscented transform with weight 1/3 at the mean [6]. We have also implemented the 3-D instrumental variable based Kalman filter (IVKF) [10]. In the considered scenario, the standard EKF and UKF do not perform well due to the high nonlinearities and the difficulty in handling the target crossing the $-\pi$ azimuth boundary and are no longer considered. In addition, we have implemented a sampling importance resampling particle filter (PF) [21] with likelihood (8)-(9) and 10000 particles.

The target state at time k is $x^k = \left[p_x^k, \dot{p}_x^k, p_y^k, \dot{p}_y^k, p_z^k, \dot{p}_z^k\right]^T$ where $\left[p_x^k, p_y^k, p_z^k\right]^T$ is its position vector and $\left[\dot{p}_x^k, \dot{p}_y^k, \dot{p}_z^k\right]^T$ is its velocity vector. The target moves with a nearly-constant velocity model

$$x^{k+1} = Fx^k + v^k, \quad F = I_3 \otimes \begin{pmatrix} 1 & \tau \\ 0 & 1 \end{pmatrix}, \qquad (38)$$

where I_3 is an identity matrix of size 3, $\otimes$ is the Kronecker product, $\tau = 0.5\,\mathrm{s}$ is the sampling time and v^k is the zero-mean process noise at time k, whose covariance matrix is

$$Q = qI_3 \otimes \begin{pmatrix} \tau^3/3 & \tau^2/2 \\ \tau^2/2 & \tau \end{pmatrix}, \qquad (39)$$

where $q = 0.25\,\mathrm{m}^2/\mathrm{s}^3$ is a parameter of the model. The prior at time 0 is Gaussian with mean $\bar{x}^0 = [-100\,(\mathrm{m}), 5\,(\mathrm{m/s}), 0\,(\mathrm{m}), 5\,(\mathrm{m/s}), 50\,(\mathrm{m}), 4\,(\mathrm{m/s})]^T$ and covariance $\Sigma^0 = \mathrm{diag}\left(\left[\sigma_{p1}^2, \sigma_{v1}^2, \sigma_{p2}^2, \sigma_{v2}^2, \sigma_{p3}^2, \sigma_{v3}^2\right]\right)$ with $\sigma_{p1}^2 = 5^2\,\mathrm{m}^2$, $\sigma_{v1}^2 = \sigma_{v2}^2 = 1\,\mathrm{m}^2/\mathrm{s}^2$, $\sigma_{p2}^2 = 150^2\,\mathrm{m}^2$, $\sigma_{p3}^2 = 4^2\,\mathrm{m}^2$, $\sigma_{v3}^2 = 0.1^2\,\mathrm{m}^2/\mathrm{s}^2$.

At each time step, the target is observed by $m = 2$ DOA sensors located at $[s_{x,1}, s_{y,1}, s_{z,1}]^T = [100, 0, 0]^T$ (m), $[s_{x,2}, s_{y,2}, s_{z,2}]^T = [-250, 0, 0]^T$ (m). Both sensor measurements are Kent-distributed with the parameters κ and β corresponding to $\sigma_\varphi^2 = (3\pi/180)^2\ \mathrm{rad}^2$ and $\sigma_\theta^2 = (1\pi/180)^2\ \mathrm{rad}^2$ and $\Gamma_j(\cdot)$ given by (32). The VMF-IPLF sets its concentration parameter to κ and disregards β.

We evaluate the filters with $J \in \{1, 5\}$ via Monte Carlo simulation with $N_{mc} = 1000$ runs and 50 different trajectories of length 100 sampled from the dynamic model. We consider multiple trajectories to compute the root mean square (RMS) position errors over different realisations of the dynamic process. The RMS position errors are shown in Figure 2. The best performing filters are K-IPLF5, K-IPLF5(T) and the PF followed by IVKF. K-IPLF1, AUKF and VMF-IPLF5. K-IPLF1(T) performs the worst. These results show the benefits of iterations and the use of sigma-points to compute the SLRs for Gaussian filters. Iterations are specially important to perform the update at the first time step due to the large uncertainty in the prior. After the initial time steps, the RMS error increases with time as the target moves away from the sensors.

The computational times (ms) to perform one Monte Carlo run on an Intel core i5 laptop are: 10 (AUKF), 6 (IVKF), 62 (VMF-IPLF(5)), 8 (K-IPLF1(T)), 32 (K-IPLF5(T)), 20 (K-IPLF1), 83 (K-IPLF5) and 450 (PF). Gaussian filters are faster than the PF. Among the Gaussian filters, the computational time is reduced by using non-iterated filters and Taylor series.

VI. Conclusions

This paper has proposed a Gaussian tracking algorithm with Kent-distributed DOA measurements with line-of-sight propagation. The Kent distribution is the spherical analogue of the bivariate Gaussian distribution and the resulting filters inherently accommodate the intrinsic characteristics of DOA data. The algorithm is based on performing iterated SLRs in the update so that the SLR is done w.r.t. the current approximation of the posterior.

We have proposed two implementations to perform the SLRs: one based on analytical linearisation and the other based on sigma-points. Performing iterated SLRs and the use of sigma-point generally improves performance. The algorithms can be directly extended when we additionally receive other types of measurements, e.g., range or Doppler [11].

The proposed Bayesian update approximation based on Kent-distributed measurements and iterated posterior linearisations is performed in a centralised manner, i.e., the algorithm directly processes all the received measurements. This approach can be directly extended to a cooperative/decentralised update using posterior linearisation belief propagation [22]. The Kent distribution and the proposed SLR approximations can also be used in other cooperative localisation approaches based on factor graphs and belief propagation [23], [24].

Future work includes the development of tracking algorithms with Kent-distributed DOA measurements subject to diffraction and non-light-of-sight propagation.

APPENDIX

To calculate (4) and (5), the procedure in [13], [17] involves the evaluation of $I_n(\kappa)$ and

$$B_n(\kappa) = \frac{I_n(\kappa)}{I_{n-2}(\kappa)}. \tag{40}$$

For large κ, the evaluation of these functions can lead to numerical problems. To improve numerical accuracy, we use the asymptotic expansion of $I_n(\kappa)$ for large κ [7, Eq. (10.3.5)]

$$I_n(\kappa) = (2\pi\kappa)^{-1/2} e^{\kappa} \left(1 - \frac{4n^2-1}{8\kappa}\right) + O\left(\kappa^{-2}\right) \tag{41}$$

such that

$$B_n(\kappa) \approx 1 + \frac{2(1-n)}{\kappa}. \tag{42}$$

The proof of (42) is as follows. Plugging (41) into (40) yields

$$\begin{aligned} B_n(\kappa) &= \frac{(2\pi\kappa)^{-1/2} e^{\kappa} \left(1 - \frac{4n^2-1}{8\kappa}\right) + O\left(\kappa^{-2}\right)}{(2\pi\kappa)^{-1/2} e^{\kappa} \left(1 - \frac{4(n-2)^2-1}{8\kappa}\right) + O\left(\kappa^{-2}\right)} \\ &= \frac{8\kappa - 4n^2 + 1}{8\kappa - 4n^2 + 16n - 15} + O\left(\kappa^{-2}\right). \end{aligned}$$

The first term of the asymptotic expansion (42) can be calculated as

$$\lim_{\kappa\to\infty} B_n(\kappa) = \frac{8\kappa - 4n^2 + 1}{8\kappa - 4n^2 + 16n - 15} = 1.$$

The factor that multiplies $1/\kappa$ in the asymptotic expansion (42) can be calculated as

$$\lim_{\kappa\to\infty} \kappa\left(B_n(\kappa) - 1\right) = -2n + 2.$$

REFERENCES

[1] D. Dardari, P. Closas, and P. M. Djuric, "Indoor tracking: Theory, methods, and technologies," *IEEE Transactions on Vehicular Technology*, vol. 64, no. 4, pp. 1263–1278, April 2015.

[2] A. Fascista, G. Ciccarese, A. Coluccia, and G. Ricci, "Angle of arrival-based cooperative positioning for smart vehicles," *IEEE Transactions on Intelligent Transportation Systems*, vol. 19, no. 9, pp. 2880–2892, Sep. 2018.

[3] Y. J. Kim and Y. S. Cho, "Beam-tracking technique for millimeter-wave cellular systems using subarray structures," *IEEE Transactions on Vehicular Technology*, vol. 67, no. 8, pp. 7806–7810, 2018.

[4] P. Tichavsky, K. T. Wong, and M. D. Zoltowski, "Near-field/far-field azimuth and elevation angle estimation using a single vector hydrophone," *IEEE Transactions on Signal Processing*, vol. 49, no. 11, pp. 2498–2510, Nov. 2001.

[5] S. Särkkä, *Bayesian Filtering and Smoothing*. Cambridge University Press, 2013.

[6] S. J. Julier and J. K. Uhlmann, "Unscented filtering and nonlinear estimation," *Proceedings of the IEEE*, vol. 92, no. 3, pp. 401–422, Mar. 2004.

[7] K. V. Mardia and P. E. Jupp, *Directional Statistics*. John Wiley & Sons, 2000.

[8] S. R. Jammalamadaka and A. SenGupta, *Topics in Circular Statistics*. World Scientific, 2001.

[9] D. F. Crouse, "Cubature/unscented/sigma point Kalman filtering with angular measurement models," in *18th International Conference on Information Fusion*, July 2015, pp. 1550–1557.

[10] N. H. Nguyen and K. Doğançay, "Instrumental variable based Kalman filter algorithm for three-dimensional AOA target tracking," *IEEE Signal Processing Letters*, vol. 25, no. 10, pp. 1605–1609, Oct. 2018.

[11] A. F. García-Fernández, F. Tronarp, and S. Särkkä, "Gaussian target tracking with direction-of-arrival von Mises-Fisher measurements," *IEEE Transactions on Signal Processing*, vol. 67, pp. 2960–2972, June 2019.

[12] J. T. Kent, "The Fisher-Bingham distribution on the sphere," *Journal of the Royal Statistical Society, Series B (Methodological)*, vol. 44, no. 1, pp. 71–80, 1982.

[13] P. Kasarapu, "Modelling of directional data using Kent distributions." [Online]. Available: https://arxiv.org/abs/1506.08105

[14] Y. F. Alem, Z. Khalid, and R. A. Kennedy, "Spherical harmonic expansion of Fisher-Bingham distribution and 3-D spatial fading correlation for multiple-antenna systems," *IEEE Transactions on Vehicular Technology*, vol. 65, no. 7, pp. 5695–5700, 2016.

[15] F. Tronarp, A. F. García-Fernández, and S. Särkkä, "Iterative filtering and smoothing in non-linear and non-Gaussian systems using conditional moments," *IEEE Signal Processing Letters*, vol. 25, no. 3, pp. 408–412, March 2018.

[16] A. F. García-Fernández, L. Svensson, M. R. Morelande, and S. Särkkä, "Posterior linearization filter: principles and implementation using sigma points," *IEEE Transactions on Signal Processing*, vol. 63, no. 20, pp. 5561–5573, Oct. 2015.

[17] D. E. Amos, "Computation of modified Bessel functions and their ratios," *Mathematics of Computation*, vol. 28, no. 125, pp. 239–251, Jan. 1974.

[18] M. R. Morelande and A. F. García-Fernández, "Analysis of Kalman filter approximations for nonlinear measurements," *IEEE Transactions on Signal Processing*, vol. 61, no. 22, pp. 5477–5484, Nov. 2013.

[19] C. E. Rasmussen and C. K. I. Williams, *Gaussian Processes for Machine Learning*. The MIT Press, 2006.

[20] J. T. Kent, I. Hussein, and M. K. Jah, "Directional distributions in tracking of space debris," in *19th International Conference on Information Fusion*, 2016, pp. 2081–2086.

[21] M. Arulampalam, S. Maskell, N. Gordon, and T. Clapp, "A tutorial on particle filters for online nonlinear/non-Gaussian Bayesian tracking," *IEEE Transactions on Signal Processing*, vol. 50, no. 2, pp. 174–188, Feb. 2002.

[22] A. F. García-Fernández, L. Svensson, and S. Särkkä, "Cooperative localization using posterior linearization belief propagation," *IEEE Transactions on Vehicular Technology*, vol. 67, no. 1, pp. 832–836, Jan. 2018.

[23] F. Meyer, O. Hlinka, and F. Hlawatsch, "Sigma point belief propagation," *IEEE Signal Processing Letters*, vol. 21, no. 2, pp. 145–149, Feb 2014.

[24] W. Yuan, N. Wu, Q. Guo, X. Huang, Y. Li, and L. Hanzo, "TOA-based passive localization constructed over factor graphs: A unified framework," *IEEE Transactions on Communications*, vol. 67, no. 10, pp. 6952–6965, 2019.